

Magnetic Property and GMI Effect of MFe_2O_4 Nanoparticles

Dao Son Lam, Ngo Thu Huong*

Faculty of Physics, VNU University of Science, 334 Nguyen Trai, Hanoi, Vietnam

Received 20 March 2017

Revised 25 April 2017; Accepted 20 June 2017

Abstract: In the present article, we report the biosensor can detect superparamagnetic nanoparticles (less than 10 nm in size) at various and low particle concentrations, which is of the importance role in biosensing applications. The nanoparticle ferrite (Fe_3O_4), Cobalt ferrite ($CoFe_2O_4$), Nickel ferrite ($NiFe_2O_4$) nanoparticles were synthesized by the high temperature thermal decomposition precursor method. The saturation of magnetization have significantly increased as the $12 \pm 1nm Fe_3O_4$ (40 emu/g), $6 \pm 0.5nm NiFe_2O_4$ (57 emu/g) and $7 \pm 0.5nm CoFe_2O_4$ (88.6 emu/g) nanoparticles. The saturation magnetization of $CoFe_2O_4$ nanoparticle is larger than $NiFe_2O_4$, Fe_3O_4 nanoparticle. The sensitivity of biosensor depend on saturation magnetization of nano particles, thus we have performed a systematic study of the longitudinally excited magneto-inductance effect of an inductive coil with $CoFe_2O_4$ nanoparticles is in its core. Our results show that the $(\Delta X/X)$ ratios and field sensitivity increase. These results are of practical importance in designing novel magnetic sensors based on the LEMI effect for sensing applications.

Keywords: Paramagnetic, magneto-reactance (MX), magneto-inductance effect.

1. Introduction

Super paramagnetic nanoparticles are very interesting materials due to their applications in magnetic resonance imaging (MRI), tissue repairing, detoxification of biological fluids, hyperthermia, drug delivery etc... Super magnetic MFe_2O_4 nanoparticles were recently made by a high-temperature reduction, decomposition reaction of metal acetylacetonate [1, 2]. Recent attention has been drawn to a new class of highly sensitive magnetic sensor based on the giant magneto impedance (GMI) effect magnetic sensors are important components in modern magneto electronic devices [3-7]. GMI effect is the change of the impedance experienced by an AC current flowing through a soft magnetic material when an external DC magnetic field is applied [3, 4]. In these reports, GMI effect displays a great potential in biosensor by adding magnetic nanoparticles [8]. GMI refers to a large change in the ac impedance $Z = R + j.X$, where R and X are the ac resistance and reactance, respectively) of a magnetic conductor subject to a dc magnetic field, and it has been observed in a number of soft

*Corresponding author. Tel.: 84-943313567.

Email: ngothuhuong2013@gmail.com

<https://doi.org/10.25073/2588-1124/vnumap.4079>

ferromagnetic materials, including magnetic wires, ribbons, and thin films [5, 9]. Further, we have demonstrated a novel method of nanoparticles detection by designing a sensing element shell that consists of multiple rounds soft ferromagnetic ribbon Co rich and its core is super magnetic nanoparticles iron oxide CoFe_2O_4 , which defined accurate concentration. The MX ratio is largest at low frequency range from 2 MHz to 6 MHz [3-9]. In our researching, the change in the inductance of the coil-system is driven by an AC current in the presence of an external dc magnetic field along the axis of the coil, producing a longitudinally excited magneto-inductance (LEMI) effect. The proposed biosensor can detect super paramagnetic nanoparticles at various low particle concentrations, which is of practical importance in biosensor applications [10]. As we known, the reactance X of the impedance component is related by the value of relatively permeability (μ). Accordingly, the induction voltage of the SEC (U_i) could be attributed to the change of the impedance Z the SEC and defined as [9]:

$$U_i \approx -NA\mu_o \left(1 + \frac{\partial M}{\partial H} \right) \frac{\partial H_{ex}}{\partial t} = -NA\mu \frac{\partial H_{ex}}{\partial t} \quad (1)$$

A: is the cross section of the SEC; N: is the turns of the SEC; μ_o : is the magnetic permeability of the vacuum; M: is the magnetization intensity of the core; H: is the magnetic field intensity which is composed by the excitation magnetic field H_{ex} and the measured magnetic field H_m ($\partial H_m / \partial T \ll \partial H_{ex} / \partial t$), μ : is the magnetic permeability in the magnetic SEC [10]. The change reactance of SEC with the applied field at a given frequency of the driving current (defined as the MX ratio) was calculated by using the following respective equations [3]:

$$\%X = \frac{X(H) - X(H_{max})}{X(H_{max})} \cdot 100 \quad (2)$$

The change MX ratio due to the presence of SPIO nanoparticles at different concentrations were obtained by subtracting the corresponding responses observed for the blank prototype as [3]:

$$\Delta\eta_\xi = [\xi]_{max,SPIO} - [\xi]_{max,Blank} \quad (3)$$

Where $[\xi]_{max}$ is the maximum values of the MX ratio in Eqs (2) respectively. This parameter is considered an important figure-of merit for assessing the sensitivity of the biosensor.

2. Experimental details

To synthesize Fe_3O_4 , CoFe_2O_4 , NiFe_2O_4 nanoparticles, we used 0.707 g of Iron (III) acetylacetonate, Cobalt (II) acetylacetonate, Nickel (II) acetylacetonate respective. They was mixed with 2.5850 g 1,2- hexadecanediol, 1.7135g oleic acid, 1.4279 g oleylamine and 20 ml benzyl ether depending on the size that we desired. We then magnetically stirred the particles while flowing argon. We heated the system to 200°C for 2 hours and 300°C for 1 hour to reflux. We then let the system cool to room temperature naturally and added 40 ml of ethanol to wash the particles. We centrifuged the resulting solution at 5000 rpm for 5 minutes, dispose of the chemical waste from process, and repeated washing by centrifugation until the liquid was clear. A Bruker AXS D8 X-ray diffractometer was used to analyze the crystalline structure of the nanoparticles, and an FEI Morgagni 268 transmission electron microscope (TEM), operating at 60 kV in Department of Physic South Florida University (USF). The magnetic properties were measured using a commercial Physical Property Measurement System (PPMS) from Quantum Design in Department of Physic, HUS-VNU.

A biosensor prototype was designed by using an amorphous micro wire of dimension diameter 1.5 μm , composition $\text{Co}_{68.2}\text{Fe}_{4.3}\text{B}_{15}\text{Si}_{12}$. These micro wires were wrapped outside the polymer tubes and the each polymer tube was used to avoid a direct contact between the SPIO nanoparticles and the ribbon surface. The sensing element coil (SEC) Co rich is about 10 mm with 50 rounds.

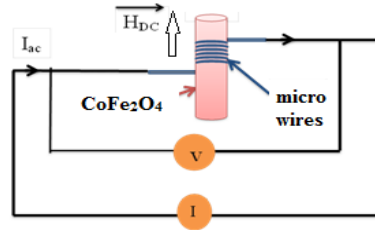


Figure 1. A schematic of the measurement system of a LEMI effect.

This polymer tube contains nanoparticles CoFe_2O_4 liquid as a magnetic sensing element. The sensing element coil (SEC) Co rich piece was fixed on a non-magnetic glass support and placed at the center of a Helmholtz coil that provided a dc magnetic field ranging up to ± 120 Oe and parallel to its length. A driving current of magnitude 5mA over the frequency range of 2,4,6 MHz was supplied along the ribbon axis, and the dc magnetic field induced MX changes were measured by a four-probe technique on a HP4192A impedance analyzer at room temperature.

To increasing of the sensitivity and of the reliability of the biosensor is an important condition of the detection of small concentration of nanoparticles. A schematic of the measurement system is displayed in Figure 1. These measurements were performed after the nanoparticles of various very low concentrations from 121.2 nM up to 1331.6 nM of CoFe_2O_4 nanoparticles liquid and compared to the measurement for a blank prototype.

3. Results and discussion

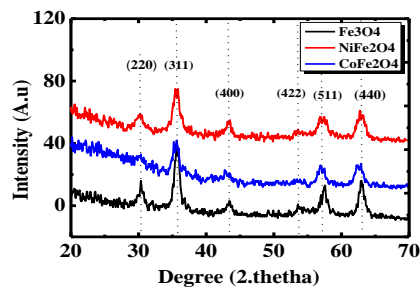


Figure 2. XRD pattern of Fe_3O_4 ; NiFe_2O_4 ; CoFe_2O_4 nanoparticles.

Fig.2 shows that the peaks at (220), (311), (400), (511) and (440) planes, which correspond to structure of nanoparticle oxides [1, 2]. This indicates that all nanoparticles above are all crystalline.

The mean crystal sizes determine by Dedye Scherre equation with XRD data have found the Fe_3O_4 , CoFe_2O_4 , NiFe_2O_4 nanoparticles, which are close to the particle size calculated from TEM images (Fig.3).

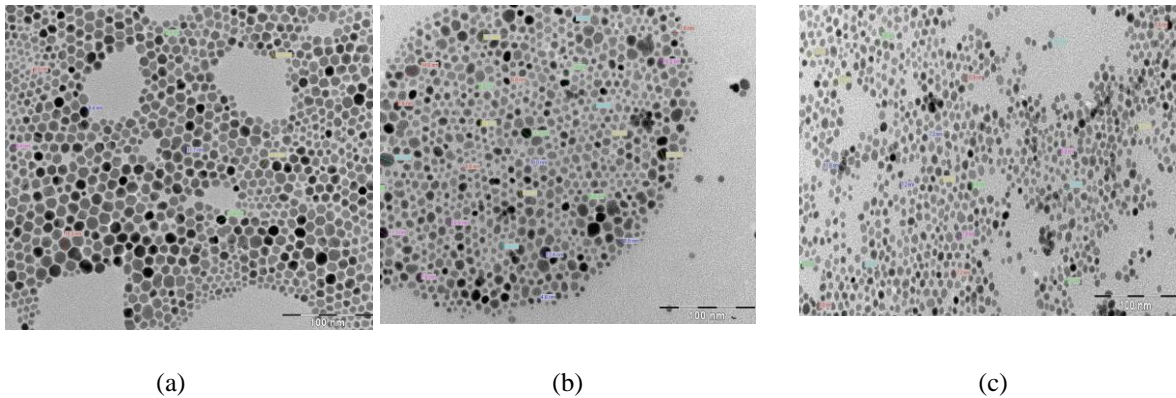


Figure 3. TEM images of the $12 \pm 1\text{nm}$ Fe_3O_4 (a), $6 \pm 0.5\text{nm}$ NiFe_2O_4 (b) $7 \pm 0.5\text{nm}$ CoFe_2O_4 (c) nanoparticles.

The super paramagnetic behavior is documented by the hysteresis loop measured at 300K as shown in figure 4. The saturation magnetization (M_s) are 88,6 emu/g for CoFe_2O_4 , 40 emu/g Fe_3O_4 , 57 emu/g for NiFe_2O_4 . The influence of Co, Ni for the spinel structure, this can exhibit by increasing the saturation magnetization values.

The magnetic saturation value of nanoparticles CoFe_2O_4 is larger than magnetic saturation of nanoparticles Fe_3O_4 , NiFe_2O_4 . Consequently in this work, we have combined CoFe_2O_4 nanoparticles and amorphous $\text{Co}_{68.2}\text{Fe}_{4.3}\text{B}_{15}\text{Si}_{12}$ material to make sensing element coil (SEC). For both samples, the GMI ratio decreased sharply with higher frequencies from 2 MHz to 6 MHz [11-14]. This can be understood by considering the corresponding contributions to the impedance from the reactance at low frequency range and the resistance at high frequency range and considering the dependence of the impedance on transverse permeability via the skin effect.

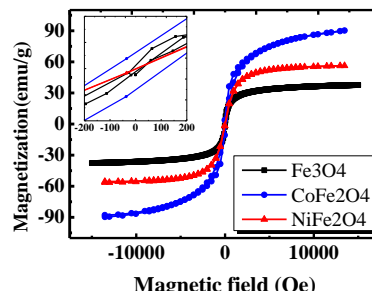


Figure 4. Magnetization curve versus applied field at 300 K for MFe_2O_4 ($M = \text{Fe, Ni, Co}$) nanoparticles.

It has been reported that magnetic losses, such as eddy current loss, hysteresis loss, ferromagnetic resonance (FMR), skin depth, etc., are important factors which must be taken into account for the decrease in X with f increase [15, 16]. A similar trend was observed for the case of the ribbon with SPIO nanoparticles, the origin of which has been well documented in our previous study [17, 18]. Amplitude of the sensor reactance (MX) can be affected by these magnetic nanoparticles added. Consequently, targeted cells can be detected and identified by the difference in MX ratio. This coupling becomes independent of SPIO nanoparticles as the concentration of nanoparticles exceeds a critical concentration (which is $\geq 621.3 \text{ nM}$ in the present case).

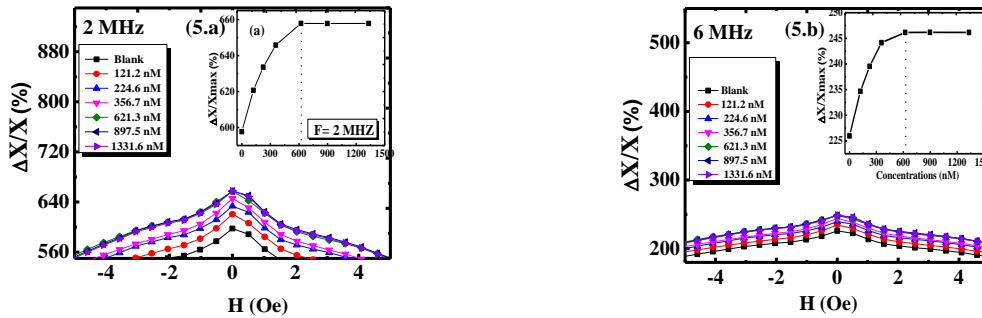


Figure 5. The DC magnetic external dependence of MX ratio ($[\Delta X/X]$) and insert maximum ($[\Delta X/X]_{\text{max}}$) for the sensing element coil samples contains various concentration nanoparticles CoFe_2O_4 at the frequency 2, 6 MHz.

The above results can be interpreted by considering the disturbance of the magnetic excitation and ac transverse fields due to the presence of the fringe magnetic fields of the SPIO nanoparticles in the sensing element coil. As the concentration of SPIO nanoparticles is increased, the strength of fringe fields also increases, thus disturbing the magnetic excitation in the sensing element to a greater degree and consequently altering the MX [8-11].

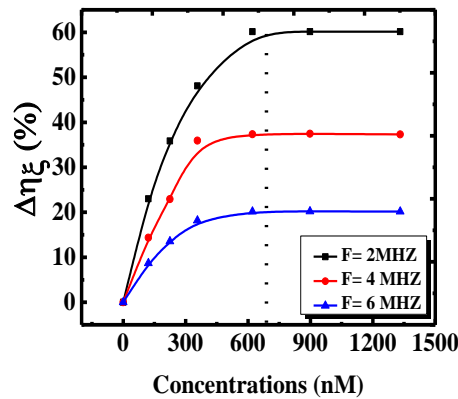


Figure 6. Relative SPIO particle concentration dependence of MX showing the sensitivity and upper limit of the detection of the biosensor at the various frequencies 2,4,6 MHz.

In the present case, the increases of MX ratio ($[\Delta X/X]$) with increasing concentration of SPIO nanoparticles (Fig. 6) can be attributed to the increase of transverse permeability due to the coupling of the magnetic fringe fields of the nanoparticles with the ac transverse magnetic field. Under an external magnetic field, the magnetic nanoparticles near the sensing element active surface develop a dipole field [6, 7, 10]. Clearly, the concentration of 621.3 nM sets an upper limit of the sensor detection of CoFe_2O_4 . Therefore, the proposed biosensor is very promising for highly sensitive detection of super paramagnetic nanoparticles as magnetic markers in biological systems.

We are now in process of exploiting this biosensor for detection and identification of different types of cancer cells that have taken up surface functionalized SPIO nanoparticles.

4. Conclusions

In this work, the MFe_2O_4 ($M = Fe, Ni, Co$) nanoparticles were successfully synthesized magnetic properties. We have performed a systematic study of the longitudinally excited magneto-inductance effect of an inductive coil with nanoparticles $CoFe_2O_4$ in its core. Our results show that the $(\Delta X/X)$ ratio and field sensitivity increase. These results are of practical importance in designing novel magnetic sensors based on the LEMI effect for sensing applications.

Acknowledgments

Research at HUS was supported by the National Foundation for Science and Technology Development of Vietnam through Grant No. 103.02-2012.69. The authors thank Prof. J.F. Sun of Harbin Institute of Technology, China for kindly providing the microwire samples.

References

- [1] Jin Xie¹, Sheng Peng, Nathan Brower, Nader Pourmand, Shan X.Wang, and Shouheng Sun, *Pure Appl. Chem.*, Vol. 78, No. 5, pp. 1003–1014, 2006.
- [2] Andrzej Skumiel, *Journal of Magnetism and Magnetic Materials* 307 (2006) 85–90
- [3] J. Devkota, T.T.T. Mai, K. Stojak, P.T. Hab, H.N. Phamb, X.P. Nguyen, P. Mukherjee, H. Srikanth, M.H. Phan, *Sensors and Actuators B* 190 (2014) 715– 722.
- [4] V. Zhukova, M. Ipatov, and A. Zhukov, *Sensors* 9, 9216 (2009).
- [5] A. Kumar, V. Fal-Miyar, J. A. Garcia, A. Cerdeira, S. Mohapatra, H. Srikanth, J. Gass, and G. V. Kurlyandskaya, *Appl. Phys. Lett.* 91, 143902 (2007).
- [6] J. Devkota, C. Wang, A. Ruiz, S. Mohapatra, P. Mukherjee, H. Srikanth, and M. H. Phan, *Journal of Applied Physics* 113, 104701 (2013).
- [7] J. Devkota, A. Ruiz, P. Mukherjee, H. Srikanth, M. H. Phan, A. Zhukov, and V. S. Larin, *J. Alloys Compd.* 549, 295 (2013).
- [8] L. Chen, C. C. Bao, H. Yang, D. Li, C. Lei, T. Wang, H. Y. Hu, M. He, Y. Zhou, and D. X. Cui, *Biosens. Bioelectron.* 26, 3246 (2011).
- [9] J. Devkota, T. Luong, J. S. Liu, H. Shen, F. X. Qin, J. F. Sun, P. Mukherjee, H. Srikanth, and M. H. Phan, *Journal of Applied Physics* 116, 234504 (2014).
- [10] Y. Geliang et al., “Design of a GMI magnetic sensor based on longitudinal excitation,” *Sens. Actuators A: Phys.*, vol. 161, pp. 72–77, 2010.
- [11] Geliang Yu, Xiongzhong Bu, Bo Yang, Yunlong Li, and Chao Xiang, *IEEE Sensor Journal*, Vol. 11, No. 10, October 2011.
- [12] M. Malatek and P. Ripka, “Single-core giant magnetoimpedance with AC Bias,” in *Proc. 5th IEEE Conf. Sensors*, 2006, pp. 1012–1015.
- [13] V. Zhukova et al., “GMI effect in ultra-thin glass-coated Co-rich amorphous wires,” *Sens. Actuators B: Chem.*, vol. 126, pp. 232–234, 2007.
- [14] Y.W. Rheem, C.G. Kim, C.O. Kim, S.S. Yoon, *Sensors and Actuators A* 106 (2003) 19–21.
- [15] Yu-Jung Cha, Ki Hyeon Kim, Jong-Sik Shon, Young Ho Kim, and Jongryoul Kim, *IEEE Transaction on magnetics*, Vol. 44, No. 11, November 2008.
- [16] Y. Zhuang, M. Vroubel, B. Rejaei, and J. N. Burghartz, *Solid-State Electron.* 51, 405 (2007). J.A.C. dePaiva, M.P.F. Graca, J. Monteiro, M.A. Macedo, M.A. Valente, 485 (2009) 637-641.
- [17] S. Mornet, S. Vasseur, F. Grasset, P. Veverka, G. Goglio, A. Demourgues, J. Portier, E. Pollert, E. Duguet, *Progress in Solid State Chemistry* 34 (2006).
- [18] Ajay Kumar Gupta, Mona Gupta, *Biomaterials* 26 (2005) 3995–4021.